Hyperfine Interactions 125 (2000) 205–221

DOS: Evaluation of phonon density of states from nuclear resonant inelastic absorption

V.G. Kohn [a] and A.I. Chumakov [b]

[a] *Russian Research Centre "Kurchatov Institute", 123182 Moscow, Russia*
[b] *European Synchrotron Radiation Facility, BP 220, F-38043 Grenoble, France*

Theoretical background and specific features of the calculation of the phonon density of states from energy spectra of nuclear resonant inelastic absorption of synchrotron radiation are presented. Double Fourier transformation is used to deconvolute data and an instrumental function and to eliminate the multiphonon contributions. A computer program is developed and an example of its work is shown.

1. Introduction

Inelastic scattering (absorption) of radiation with creation or annihilation of phonons provides powerful techniques to study lattice dynamics. For example, neutron, X-ray and light inelastic scattering have long been used to determine the phonon dispersion law $\omega_j(\mathbf{q})$, where $\hbar\omega$ is the energy and $\mathbf{q}$ is the wave vector. In conventional Mössbauer spectroscopy lattice dynamics is probed only by the f-factor, the probability of the occurrence of the Mössbauer effect. The progress in nuclear resonant scattering of synchrotron radiation [1] together with the development of high-resolution X-ray monochromators [2] allowed one to measure energy spectra of nuclear resonant inelastic absorption directly. A review of relevant experiments may be found in [3].

A theory of nuclear inelastic absorption [4] was developed long before successful experiments were performed. It was shown that the energy spectrum of nuclear inelastic absorption may be decomposed into single-phonon and multiphonon contributions. The single-phonon contribution is determined directly by the phonon density of states (DOS) for single crystals with a cubic Bravais lattice. The same result is obtained for polycrystalline samples, which are composed of only resonant atoms.

For more complicated single crystals the single-phonon contribution depends on the orientation of the incident beam relative to the crystal lattice [5]. The theory of inelastic nuclear absorption in single crystals was developed in [6] (see also [7]). It was shown that inelastic absorption is not defined by the true DOS, but the function which additionally contains a term dependent on the square modulus of the projection of the phonon polarization vector for resonant atoms on the direction of the incident beam. This function was called the projected density of states (PDOS) [6].

The calculation of the PDOS from the energy spectra of nuclear resonant inelastic absorption is performed in two steps. First, one has to separate the single-phonon absorption term from multiphonon contributions. In a first approximation, the multiphonon contributions may be eliminated using recursive procedures [3]. However, the PDOS obtained is not the true one, but convoluted with an instrumental function of the monochromator. Thus, the second step deals with the deconvolution of the data and the instrumental function. In fact, both problems may be addressed simultaneously using the method of double Fourier transformation [6], which allows one to eliminate the multiphonon contribution together with the deconvolution of the data.

This work is devoted to a detailed description of computational aspects of extracting PDOS from the measured spectra of inelastic nuclear absorption. First, the theory in the case of an incident monochromatic wave is reviewed briefly. Then the deconvolution of the data and the instrumental function as well as the problem of noise dumping is discussed. Finally, the principles of the computer implementation and the program structure are shown together with an example of the program performance.

2. The theory of nuclear inelastic absorption

A general expression for the X-ray absorption cross-section per nucleus in terms of a time integral was obtained by Singwi and Sjölander [4]. We use this expression without derivation. We assume that the phonon energy is much larger than a possible hyperfine splitting of the nuclear levels. Therefore, the hyperfine structure can be neglected. We consider in an explicit form a crystal with a complex unit cell, which may contain several different atoms as well as several identical atoms at various positions. However, we will not distinguish resonant nuclei in the unit cell, because this is impossible in an experiment, and assume that there is only one resonant nucleus inside the unit cell. If this is not the case the average value is considered.

We introduce a normalized probability of absorption $W(E)$ per unit energy interval at the energy E. Equation (2) of the article of Singwi and Sjölander can be rewritten as

$$W(E) = \int \frac{\mathrm{d}\tau}{2\pi} \exp\left(-\mathrm{i}E\tau - \frac{\Gamma}{2}|\tau|\right) F(\mathbf{k}, \tau), \tag{2.1}$$

where $\tau = t/\hbar$, t is the time, Γ is the natural width of the excited nuclear state, E is the difference between the energy of the γ-ray and the resonance energy of the nuclear transition, $\mathbf{k}$ is the wave vector of the incident γ-ray. The function

$$F(\mathbf{k}, \tau) = \big\langle \exp\big(-\mathrm{i}\mathbf{k}\mathbf{u}(0)\big) \exp\big(\mathrm{i}\mathbf{k}\mathbf{u}(\tau)\big)\big\rangle \tag{2.2}$$

is the time-dependent correlation function, which describes the correlation between the displacement $\mathbf{u}$ of the nucleus at two different moments of time separated by the time interval $t = \hbar\tau$. In a single crystal this function has a translational symmetry.

In order to deal with this function, Singwi and Sjölander introduced the Van Hove space–time correlation function $G_\mathrm{s}(\mathbf{r}, t)$ in a spherically symmetrical approximation, which is valid for polycrystals and crystals with a cubic Bravais lattice. In this way the dependence on the direction of the photon beam is lost. However, it is not necessary to consider the space–time correlation function $G_\mathrm{s}(\mathbf{r},t)$ for the calculation of $F(\mathbf{k},\tau)$. As shown by Van Hove [8] (see eq. (51) of his article), this function can be presented in the general case of an anisotropic crystal as

$$F(\mathbf{k},\tau) = \exp\bigl(-Z(\mathbf{k})\bigr)\exp\bigl(M(\mathbf{k},\tau)\bigr), \tag{2.3}$$

where

$$Z(\mathbf{k}) = M(\mathbf{k},0) = \frac{E_\mathrm{R}}{N}\sum_{\mathbf{q}j}\frac{|\mathbf{s}\cdot\mathbf{e}_j(\mathbf{q})|^2}{\hbar\omega_j(\mathbf{q})}\bigl(2\overline{n}_{\mathbf{q}j}+1\bigr), \tag{2.4}$$

$$M(\mathbf{k},\tau) = \frac{E_\mathrm{R}}{N}\sum_{\mathbf{q}j}\frac{|\mathbf{s}\cdot\mathbf{e}_j(\mathbf{q})|^2}{\hbar\omega_j(\mathbf{q})}\bigl[\bigl(\overline{n}_{\mathbf{q}j}+1\bigr)\exp\bigl(\mathrm{i}\hbar\omega_j(\mathbf{q})\tau\bigr)+\overline{n}_{\mathbf{q}j}\exp\bigl(-\mathrm{i}\hbar\omega_j(\mathbf{q})\tau\bigr)\bigr]. \tag{2.5}$$

Equations (2.3)–(2.5) extend the Van Hove formulas to the general case of a noncubic Bravais crystal lattice. The derivation is similar to that given by Van Hove and we omit it here. In formulas (2.4), (2.5), $E_\mathrm{R} = \hbar^2k^2/2M$ is the recoil energy; M is the mass of a nucleus; N is the number of unit cells per unit volume of the crystal; $\omega_j(\mathbf{q})$ is the phonon dispersion relation for the branch j; $\mathbf{e}_j(\mathbf{q})$ is the polarization vector of the vibrations for the resonant atom in the mode $\{\mathbf{q}j\}$; $\mathbf{s} = \mathbf{k}/k$;

$$\overline{n}_{\mathbf{q}j} = \bigl[\exp\bigl\{\beta\hbar\omega_j(\mathbf{q})\bigr\}-1\bigr]^{-1} \tag{2.6}$$

is the Bose–Einstein distribution function, $\beta = (k_\mathrm{B}T)^{-1}$; k_B is the Boltzmann constant, and T is the temperature. We note that $\exp(-Z(\mathbf{k})) \equiv f_\mathrm{LM}(\mathbf{k})$ is the angle-dependent Lamb–Mössbauer factor.

In order to calculate the integral in eq. (2.1), we expand the exponent $\exp(M(\mathbf{k},\tau))$ in a power series and arrive at the expansion $W(E) = \sum_{n=0}^{\infty} W_n(E)$, where each term $W_n(E)$ corresponds to photon absorption accompanied by creation or annihilation of n phonons.

The zero term of this expansion describes elastic nuclear absorption without phonon creation or annihilation. It can be calculated directly using

$$\int\frac{\mathrm{d}\tau}{2\pi}\exp\biggl(-\mathrm{i}E\tau-\frac{\Gamma}{2}|\tau|\biggr) = \frac{1}{2\pi}\frac{\Gamma}{(E^2+\Gamma^2/4)} = \delta_\Gamma(E) \tag{2.7}$$

as

$$W_0(E) = \delta_\Gamma(E)f_\mathrm{LM}(\mathbf{k}), \quad \lim_{\Gamma\to 0}\delta_\Gamma(E) = \delta(E), \tag{2.8}$$

where $\delta(E)$ is the Dirac δ-function.

The first term describes a single-phonon nuclear inelastic absorption. It is calculated by the same integral (2.7), however, the result has a more complicated form:

$$W_1(E) = \frac{E_\mathrm{R}}{N} f_\mathrm{LM}(\mathbf{k}) \sum_{\mathbf{q}j} \frac{|\mathbf{s}\cdot\mathbf{e}_j(\mathbf{q})|^2}{\hbar\omega_j(\mathbf{q})} \\ \times \left[\left(\overline{n}_{\mathbf{q}j}+1\right)\delta_\Gamma\left(E-\hbar\omega_j(\mathbf{q})\right) + \overline{n}_{\mathbf{q}j}\,\delta_\Gamma\left(E+\hbar\omega_j(\mathbf{q})\right)\right]. \tag{2.9}$$

After replacement of $\delta_\Gamma(E)$ by $\delta(E)$ and taking into account that $\overline{n}_{\mathbf{q}j}$ depends only on $\hbar\omega_j(\mathbf{q})$ (see eq. (2.6)), expression (2.9) becomes

$$W_1(E) = f_\mathrm{LM}(\mathbf{k}) S^{(1)}(E,\mathbf{k}), \quad S^{(1)}(E,\mathbf{k}) = \frac{E_\mathrm{R}\, g(|E|\mathbf{s})}{E(1-\exp(-\beta E))}. \tag{2.10}$$

The form of this expression is similar to that used by Singwi and Sjölander [4]. However, the dependence of the absorption probability on the direction of the incident photon beam relative to the crystal lattice is obtained in an explicit form:

$$g(E,\mathbf{s}) = V_0 \sum_j \int \frac{\mathrm{d}\mathbf{q}}{(2\pi)^3} \delta\left(E-\hbar\omega_j(\mathbf{q})\right)\left|\mathbf{s}\cdot\mathbf{e}_j(\mathbf{q})\right|^2 \\ = \frac{V_0}{(2\pi)^3} \sum_j \int \frac{\mathrm{d}q_1\,\mathrm{d}q_2}{|\mathrm{grad}_\mathbf{q}\hbar\omega_j(\mathbf{q})|} \left|\mathbf{s}\cdot\mathbf{e}_j(\mathbf{q})\right|^2. \tag{2.11}$$

Here $V_0 = 1/N$ is the volume of the unit cell. We have passed from a sum to an integral according to the usual technique. The integral is taken over the surface of constant energy $\hbar\omega_j(\mathbf{q}) = E$ in the **q**-space within the first Brillouin zone. The coordinates q_1 and q_2 are the axes of the local Cartesian system of reference. These lie on the surface of constant energy E. The third axis q_3 of the Cartesian system is directed along the vector $\mathrm{grad}_\mathbf{q}\hbar\omega_j(\mathbf{q})$.

The function $g(E,\mathbf{s})$ coincides with the conventional phonon density of states (DOS) for single crystals with a cubic Bravais lattice. The same result may be obtained for polycrystalline samples, which are composed of only resonant atoms. In this case averaging over all directions of the incident beam and summing over atoms leads to the expression

$$g(E) = \frac{1}{3n_\mathrm{c}} V_0 \sum_j \int \frac{\mathrm{d}\mathbf{q}}{(2\pi)^3} \delta\left(E-\hbar\omega_j(\mathbf{q})\right), \tag{2.12}$$

where n_c is the number of atoms inside the unit cell. However, in the general case of a single crystal the function $g(E,\mathbf{s})$ does not coincide with the DOS. In contrast to the DOS, it contains contributions of phonons weighted by the projection of their polarization vectors for resonant atoms on the direction of the X-ray beam. Therefore, we will call this function the projected density of states (PDOS). As shown below, this function is normalized to unity for any direction of **s**.

Considering the higher-order terms of the multiphonon expansion, we omit the energy width Γ of the nuclear levels, which is negligible compared to the phonon energy, and rewrite eq. (2.1),

$$W_n(E) = f_{\mathrm{LM}}(\mathbf{k})\, S^{(n)}(E,\mathbf{k}), \tag{2.13}$$

where

$$S^{(n)}(E,\mathbf{k}) = \int \frac{\mathrm{d}\tau}{2\pi} \exp(-\mathrm{i}E\tau)\, \frac{M(\mathbf{k},\tau)}{n}\, \frac{(M(\mathbf{k},\tau))^{n-1}}{(n-1)!}. \tag{2.14}$$

The integral in eq. (2.14) is the Fourier image of the product of two functions. It can be represented as the convolution of the Fourier images of these functions. This leads to the recursive relation

$$S^{(n)}(E,\mathbf{k}) = \frac{1}{n} \int \mathrm{d}E'\, S^{(1)}\big(E',\mathbf{k}\big) S^{(n-1)}\big(E-E',\mathbf{k}\big), \tag{2.15}$$

which permits the calculation of the multiphonon scattering cross-section from the single-phonon term.

As a result we obtain the expression for the probability of nuclear absorption in a form similar to the formula obtained by Singwi and Sjölander:

$$W(E,\mathbf{k}) = f_{\mathrm{LM}}(\mathbf{k}) \left(\delta_\Gamma(E) + \sum_{n=1}^{\infty} S^{(n)}(E,\mathbf{k}) \right). \tag{2.16}$$

In our case, however, the explicit dependence of nuclear absorption on the direction **k** of the photon propagation relative to the crystal lattice is revealed through the projected density of the phonon state $g(E,\mathbf{s})$.

In order to calculate the Lamb–Mössbauer factor we note that

$$S^{(1)}(E,\mathbf{k}) = \int \frac{\mathrm{d}\tau}{2\pi} \exp(-\mathrm{i}E\tau) M(\mathbf{k},\tau). \tag{2.17}$$

Therefore

$$M(\mathbf{k},\tau) = \int \mathrm{d}E\, \exp(\mathrm{i}E\tau) S^{(1)}(E,\mathbf{k}). \tag{2.18}$$

Now from (2.4) and (2.10) we obtain the Lamb–Mössbauer factor as

$$f_{\mathrm{LM}}(\mathbf{k}) = \exp\left(-E_{\mathrm{R}} \int_0^{\infty} \mathrm{d}E\, g(E,\mathbf{s}) E^{-1} \frac{1+\exp(-\beta E)}{1-\exp(-\beta E)} \right). \tag{2.19}$$

We see that the Lamb–Mössbauer factor in an anisotropic crystal is completely determined by the PDOS.

3. Lipkin's sum rules

The sum rules given by Lipkin [9] have proved to be a useful tool to treat the data on inelastic nuclear absorption, because they simplify the normalization of the experimental spectra. Therefore, it is worthwhile to derive them in the general case of an anisotropic single crystal. We rewrite eq. (2.1) as

$$W(E) = \int \frac{\mathrm{d}\tau}{2\pi} \exp(-\mathrm{i}E\tau)\Phi(\tau) = \frac{1}{E^n} \int \frac{\mathrm{d}\tau}{2\pi} \exp(-\mathrm{i}E\tau)\left(\frac{\mathrm{d}^n\Phi(\tau)}{\mathrm{i}^n\,\mathrm{d}\tau^n}\right), \tag{3.1}$$

where

$$\Phi(\tau) = \exp\left(-\frac{\Gamma}{2}|\tau|\right) F(\mathbf{k}, \tau) \tag{3.2}$$

is the Fourier image of the energy spectrum of the absorption probability. The right-hand side of eq. (3.1) is obtained by integration by parts taking into account that $\Phi(\tau)$ and its derivatives go to zero as $|\tau| \to \infty$.

We shall use the notation $\langle E^n \rangle_A = \int_{-\infty}^{\infty} \mathrm{d}E\, A(E) E^n$ for the nth moment of the function $A(E)$. The zero moment of the absorption probability is

$$\langle E^0 \rangle_W = \int \mathrm{d}E\, W(E) = \Phi(0) = 1, \tag{3.3}$$

which follows immediately from the left-hand sides of eqs. (3.1) and (2.3). This proves the correct normalization of the absorption probability in eq. (2.1).

The first moment can be easily calculated from the right-hand side of eq. (3.1) for $n = 1$, namely,

$$\langle E^1 \rangle_W = \int \mathrm{d}E\, W(E) E = \left(\frac{\mathrm{d}\Phi(\tau)}{\mathrm{i}\,\mathrm{d}\tau}\right)_{\tau=0} = \left(\frac{\mathrm{d}M(\mathbf{k},\tau)}{\mathrm{i}\,\mathrm{d}\tau}\right)_{\tau=0}. \tag{3.4}$$

Substitution of eq. (2.5) gives

$$\begin{aligned}\langle E^1 \rangle_W &= \frac{E_\mathrm{R}}{N} \sum_{\mathbf{q}j} \frac{|\mathbf{s} \cdot \mathbf{e}_j(\mathbf{q})|^2}{\mathrm{i}\hbar\omega_j(\mathbf{q})} \left[\mathrm{i}\hbar\omega_j(\mathbf{q})\big(\overline{n}_{\mathbf{q}j} + 1\big) - \mathrm{i}\hbar\omega_j(\mathbf{q})\overline{n}_{\mathbf{q}j}\right] \\ &= \frac{E_\mathrm{R}}{N} \sum_{\mathbf{q}j} \left|\mathbf{s} \cdot \mathbf{e}_j(\mathbf{q})\right|^2 = E_\mathrm{R}. \end{aligned} \tag{3.5}$$

Thus, we obtain Lipkin's sum rule: the first energy moment of the probability of nuclear absorption is equal to the recoil energy E_R of a free nucleus.

The higher-order energy moments can be calculated similarly. For example, the second energy moment of the absorption probability is

$$\langle E^2 \rangle_W = \int \mathrm{d}E\, W(E) E^2 = \left(-\frac{\mathrm{d}^2\Phi(\tau)}{\mathrm{d}\tau^2}\right)_{\tau=0}. \tag{3.6}$$

We note that this moment diverges if the integral is taken over an infinite energy interval. The divergence results from the property of the function $\delta_\Gamma(E)$, which is not exactly the δ-function but behaves like E^{-2} in the tails. However, in practice we handle data taken over the finite energy range of $2E_\mathrm{max}$, where E_max is larger than the phonon energy but much smaller than $\langle E^2 \rangle/\Gamma$. This allows us to neglect the tails, performing the integration and treat $\delta_\Gamma(E)$ as the exact δ-function for all energies considered. In this approximation we obtain

$$\begin{aligned}\langle E^2\rangle_W &= E_\mathrm{R}^2 + \frac{E_\mathrm{R}}{N}\sum_{\mathbf{q}j}\left|\mathbf{s}\cdot\mathbf{e}_j(\mathbf{q})\right|^2\hbar\omega_j(\mathbf{q})(2\overline{n}_{\mathbf{q}j}+1)\\ &= E_\mathrm{R}^2 + E_\mathrm{R}\int_0^\infty \mathrm{d}E\, g(E,\mathbf{s})\,E\,\frac{1+\exp(-\beta E)}{1-\exp(-\beta E)}.\end{aligned}\tag{3.7}$$

In order to obtain this expression we multiplied the right-hand side by unity in the form $\int_0^\infty \mathrm{d}E\,\delta(E-\hbar\omega_j(\mathbf{q}))$ and performed the integration. We note that eq. (3.7) can be rewritten as

$$\frac{\langle E^2\rangle_W - E_\mathrm{R}^2}{4E_\mathrm{R}} = \frac{1}{2}\int_0^\infty \mathrm{d}E\,E\,g(E,\mathbf{s})\left[n(E)+\frac{1}{2}\right] = \langle T(\mathbf{s})\rangle,\tag{3.8}$$

where $\langle T(\mathbf{s})\rangle$ is the mean kinetic energy per phonon along the direction $\mathbf{s}$, as shown by Lipkin [9].

Using the same approximation, one may consider the higher energy moments. For example,

$$\langle E^3\rangle_W = 3E_\mathrm{R}\langle E^2\rangle_W - 2E_\mathrm{R}^3 + E_\mathrm{R}\int_0^\infty \mathrm{d}E\,g(E,\mathbf{s})E^2.\tag{3.9}$$

This value determines the mean force constant $\langle F\rangle$ according to Lipkin [9]:

$$\frac{M}{\hbar^2 E_\mathrm{R}}\left[\langle E^3\rangle_W - 3E_\mathrm{R}\langle E^2\rangle_W + 2E_\mathrm{R}^3\right] = \frac{M}{\hbar^2}\int_0^\infty \mathrm{d}E\,g(E,\mathbf{s})E^2 = \langle F\rangle.\tag{3.10}$$

We note that the probability of elastic nuclear absorption $W_0(E)$ as determined by eq. (2.8) leads to the zero moment $\langle E^0\rangle_{W_0} = f_\mathrm{LM}(\mathbf{k})$, whereas all other moments are zero. Therefore, relations (3.5), (3.7) and (3.9) hold for the inelastic part of nuclear absorption $W(E)-W_0(E)$ as well.

4. The method of PDOS calculation

4.1. General procedure

Here we consider the method of calculating PDOS from the experimental data. PDOS is obtained from the single-phonon term of inelastic absorption. Therefore, this term has to be separated from elastic and multiphonon contributions. Besides that, the experimental data are influenced by the finite energy bandwidth of the X-ray beam, whereas in the discussion above we have assumed monochromatic radiation. Therefore, it is necessary to examine the application of Lipkin's sum rules to the experimental energy spectra and to consider the deconvolution of the data and the instrumental function.

Let $P_m(E)$ be the normalized energy distribution of the quanta in the X-ray beam (instrumental function of the monochromator). We have to exclude the elastic part of the incoherent absorption spectrum from our analysis because in this case the theory is not adequate for the experiment. The reason is that the theory does not take into account a possible strong coherent channel of scattering that may lead to a faster decay of the synchrotron pulse. However, the experiment is performed with a well collimated beam and the coherent elastic forward scattering is really strong and influences the wave field significantly. Therefore, we consider only the inelastic part of the absorption, $W_{\mathrm{inel}}(E) = W(E) - W_0(E)$. The experimental energy spectrum $I(E,\mathbf{k})$ can be represented as follows:

$$\begin{aligned} I(E,\mathbf{k}) &= I_0 \int \mathrm{d}E' P(E') W_{\mathrm{inel}}(E-E',\mathbf{k}) \\ &= I_0 f_{\mathrm{LM}}(\mathbf{k}) \int \frac{\mathrm{d}\tau}{2\pi} \exp\left(-\mathrm{i}E\tau - \frac{\Gamma}{2}|\tau|\right) Q(\tau)\left[\exp(M(\mathbf{k},\tau) - 1\right]. \end{aligned} \tag{4.1}$$

Here I_0 is a scaling factor and $Q(\tau)$ is the Fourier image of $P(E) = P_m(-E)$. It is evident that $Q(\tau) = \int \mathrm{d}E \exp(\mathrm{i}E\tau)P(E)$ has a peak with a characteristic width w which satisfies the inequality $w \gg \Gamma$. For example, if $P(E)$ is a Gaussian with the standard deviation (root mean square – rms) σ, then $Q(\tau)$ is also a Gaussian with the rms σ^{-1}:

$$\begin{aligned} P(E) &= \frac{1}{\sigma\sqrt{2\pi}} \exp\left(-\frac{E^2}{2\sigma^2}\right), \\ Q(\tau) &= \int \mathrm{d}E \exp(\mathrm{i}E\tau)P(E) = \exp\left(-\frac{\tau^2}{2\sigma^{-2}}\right). \end{aligned} \tag{4.2}$$

Therefore, we may again consider the limit $\Gamma \to 0$ and omit the term containing Γ.

The contribution of single-phonon absorption to the experimental data is

$$\begin{aligned} I_1(E,\mathbf{k}) &= I_0 f_{\mathrm{LM}}(\mathbf{k}) \int \mathrm{d}E' P(E') S_1(E-E',\mathbf{k}), \\ S_1(E,\mathbf{k}) &= \frac{E_{\mathrm{R}}\, g(|E|,\mathbf{s})}{E(1-\exp(-\beta E))}. \end{aligned} \tag{4.3}$$

We may assume here that the function $E^{-1}(1-\exp(-\beta E))^{-1}$ varies slowly within the energy band selected by the monochromator. This leads to the approximate formula

$$I_1(E,\mathbf{k}) = I_0 f_{\mathrm{LM}}(\mathbf{k}) \frac{E_{\mathrm{R}}\overline{g}(|E|,\mathbf{s})}{E(1-\exp(-\beta E))}, \tag{4.4}$$

where

$$\begin{aligned} \overline{g}(E,\mathbf{s}) &= \int \mathrm{d}E' P(E') g(E-E',\mathbf{s}) \\ &= V_0 \sum_j \int \frac{\mathrm{d}\mathbf{q}}{(2\pi)^3} P(E - \hbar\omega_j(\mathbf{q})) \left|\mathbf{s}\cdot\mathbf{e}_j(\mathbf{q})\right|^2. \end{aligned} \tag{4.5}$$

This function is a smoothed PDOS, where the δ-function is replaced by the energy spectrum of the monochromator. This smoothing may be destructive because the function $g(E, \mathbf{s})$, in general, is not a slowly varying function. It may contain sharp peaks if the phonon dispersion branches have plane areas on the surface $\omega_j(\mathbf{q})$ in $\mathbf{q}$ space with a small value of $|\mathrm{grad}_{\mathbf{q}} \hbar\omega_j(\mathbf{q})|$. In these cases the deconvolution procedure is desirable.

Considering the higher-order terms, we note that the recursive relation (2.15), which was obtained for the multiphonon contributions to the absorption probability $S^{(n)}(E, \mathbf{k})$, is not valid for $I_n(E, \mathbf{k})$. Therefore, procedures which use relation (2.15) in order to eliminate the multiphonon terms from the experimental data are, in general, not exact. Our program uses a quite different approach, which allows one to separate the single-phonon term from multiphonon contributions simultaneously with the deconvolution of the data and the instrumental function.

In the first step, we determine the scaling factor I_0. For this purpose we apply the sum rules. The zero and first moments of the experimental energy spectrum are given by

$$\langle E^0\rangle_I = \int \mathrm{d}E\, I(E, \mathbf{k}) = I_0\bigl(1 - f_{\mathrm{LM}}(\mathbf{k})\bigr), \tag{4.6}$$

$$\langle E^1\rangle_I = \int \mathrm{d}E\, I(E, \mathbf{k})E = \langle E^0\rangle_I \langle E^1\rangle_P + I_0\, E_{\mathrm{R}}. \tag{4.7}$$

Here we use $\langle E^0\rangle_P = Q(0) = \int \mathrm{d}E\, P(E) = 1$, because the instrumental function is normalized. It can, however, be asymmetric, and then the first moment of $P(E)$ differs from zero. From eqs. (4.6), (4.7) we obtain I_0 and $f_{\mathrm{LM}}(\mathbf{k})$:

$$I_0 = \frac{(\langle E^1\rangle_I - \langle E^0\rangle_I \langle E^1\rangle_P)}{E_{\mathrm{R}}}, \qquad f_{\mathrm{LM}}(\mathbf{k}) = 1 - \frac{\langle E^0\rangle_I}{I_0}. \tag{4.8}$$

In the next step, we calculate the function $M(\mathbf{k}, \tau)$ directly from the experimental energy spectrum using a Fourier transformation:

$$M(\mathbf{k}, \tau) = \ln\bigl(1 + J(\mathbf{k}, \tau)\bigr), \tag{4.9}$$

$$J(\mathbf{k}, \tau) = \frac{\int \mathrm{d}E \exp(\mathrm{i}E\tau) I(E, \mathbf{k})}{I_0 f_{\mathrm{LM}}(\mathbf{k}) Q(\tau)}. \tag{4.10}$$

Finally, we perform the reverse Fourier transformation and obtain the projected density of phonon states:

$$\begin{aligned} D(E, \mathbf{s}) &= \frac{E}{E_{\mathrm{R}}}\bigl(1 - \exp(-\beta E)\bigr) \int \frac{\mathrm{d}\tau}{2\pi} \exp(-\mathrm{i}E\tau) M(\mathbf{k}, \tau), \\ g(E, \mathbf{s}) &= D(E, \mathbf{s}), \quad E > 0. \end{aligned} \tag{4.11}$$

We note that eq. (4.9) allows one to calculate the single-phonon term (without the multiphonon processes) simply as the logarithm of $1 + J(\mathbf{k}, \tau)$ after deconvolution of the data and the instrumental function according to eq. (4.10).

In addition, we may verify the reliability of the experimental data and check the procedure of their treatment. For this purpose we derive several relations, which connect the various energy moments of the experimental data with those of the DOS. It is convenient to write them as conditions for the function

$$G_n(\mathbf{s}) = \int_0^\infty \mathrm{d}E\, g(E,\mathbf{s})E^n \frac{1+C_n(E)}{1-C_n(E)}, \quad C_n(E) = \frac{1-(-1)^n}{2}\exp(-\beta E). \tag{4.12}$$

From the equations obtained above we have

$$G_{-1}(\mathbf{s}) = \frac{1}{E_\mathrm{R}} \ln\left(\frac{1}{f_\mathrm{LM}(\mathbf{k})}\right), \qquad G_0(\mathbf{s}) = \int_0^\infty \mathrm{d}E\, g(E,\mathbf{s}) = 1, \tag{4.13}$$

$$G_1(\mathbf{s}) = E_\mathrm{R}^{-1}\langle E^2\rangle_W - E_\mathrm{R}, \qquad G_2(\mathbf{s}) = E_\mathrm{R}^{-1}\langle E^3\rangle_W - 3\langle E^2\rangle_W + 2E_\mathrm{R}^2, \tag{4.14}$$

where the moments of the probability density are connected with the measured data as

$$\langle E^2\rangle_W = I_0^{-1}\left(\langle E^2\rangle_I - \langle E^2\rangle_P\langle E^0\rangle_I\right) - 2\langle E^1\rangle_P E_\mathrm{R}, \tag{4.15}$$

$$\langle E^3\rangle_W = I_0^{-1}\left(\langle E^3\rangle_I - \langle E^3\rangle_P\langle E^0\rangle_I\right) - 3\langle E^1\rangle_P\langle E^2\rangle_W - 3\langle E^2\rangle_P E_\mathrm{R}. \tag{4.16}$$

Conditions (4.13) and (4.14) can be used for the verification of the experimental results. In particular, eq. (4.13) compares the Lamb–Mössbauer factor obtained from the area of the inelastic part of the normalized experimental energy spectrum with that calculated from the retrieved PDOS and verifies the normalization of PDOS.

Another possibility to examine the reliability of the experimental data is to compare $D(E,\mathbf{s})$ (eq. (4.11)) for positive and negative values of E. The part with $E > 0$ describes the DOS that is determined from the processes of phonon absorption, while the part with $E < 0$ describes the DOS from the processes of phonon creation. Both parts must be equal, $D(-E,\mathbf{s}) = D(E,\mathbf{s})$. In fact, it is more accurate to calculate the density of phonon states from the positive part, because the phonon absorption has a higher statistical accuracy.

4.2. Computer realization

4.2.1. Correction of the experimental data

In order to check the sensitivity of the data to possible experimental errors, the initial experimental spectrum $I_t^{(i)}(E)$ may be corrected in the program using

$$I_t(E) = I_t^{(i)}(E)[1 + A_\mathrm{p}E]. \tag{4.17}$$

Here A_p is a parameter of the program. Conventionally, A_p should be set to zero.

4.2.2. Noise dumping

The procedure of extracting the instrumental function by means of a Fourier transformation is very sensitive to noise in the experimental data. A crucial condition is that the amplitudes of the high frequency components of the spectrum must be smaller than those of the instrumental function. This condition may be violated in practice, because both the experimental spectrum and the instrumental function contain random deviations of the measured values from the real ones due to the finite statistics of the measurements. Moreover, usually the experimental spectrum has a statistical accuracy less than that of the instrumental function.

Therefore, the computer program, in general, cannot work with the raw data because the noise may give false peaks in the PDOS. An additional problem is that noise masks the small real peaks of the experimental spectra which correspond to significant peaks of PDOS. In order to solve this problem, there must be a special filter in the program that allows one to eliminate the noise. This procedure cannot work automatically, because it depends significantly on the quality of the data.

The filter consists of the procedures described below. In the first step, the data are condensed from groups of channels to one channel. The number of summed channels is different in various parts of the spectrum. The initial number of channels is set by the parameter N_{si}. However, if the maximum deviation of the value for each channel from the mean value for the channels under consideration exceeds the parameter P^{i}_{rms}, this number is reduced to satisfy that condition. In the regions of strong changes of the curve, the number of channels to be summed may be reduced to 1 (no summation). The same procedure for the instrumental function uses a parameter P^{m}_{rms} while the parameter N_{si} is the same.

In the next step, the data are interpolated to a constant step array for Fast Fourier Transformation (FFT). In order to avoid large deviations, a linear interpolation is used. The FFT procedure uses the finite energy region $-E_b < E < E_b$, where E_b is a parameter of the program. The number of channels for FFT must be $N = 2^n$ (n integer). This number is also a parameter of the program. The user may choose between $N = 2048$, 4096 and 8192. The experimental data do not cover the total energy region for FFT. Therefore, the tails of the experimental curve are linearly extrapolated to zero within an interval of N_b channels, where N_b is a parameter of the program.

Finally, in order to smooth the data, the values of all channels are replaced by new values, each of them calculated as the mean value for neighbouring N_m channels. N_m is a parameter of the program.

4.2.3. Subtraction of the central peak of elastic scattering

The scheme described above cannot be used directly for a computer calculation. The first problem is the subtraction of the elastic part from the total spectrum:

$$I_t(E,\mathbf{k}) = I_0 \int \mathrm{d}E' P\bigl(E'\bigr) W_0\bigl(E-E',\mathbf{k}\bigr) + I(E,\mathbf{k}). \qquad (4.18)$$

For this purpose we calculate all energy moments of the total intensity I_t as well as the energy moments of the instrumental function. Then the normalization constant I_0 is calculated from the first moment using the corresponding sum rule for the total intensity:

$$I_0 = \frac{\langle E^1\rangle_{It} - \langle E^0\rangle_{It}\langle E^1\rangle_P}{E_{\rm R}}. \tag{4.19}$$

Here the instrumental function is assumed to be normalized. After that, the spectrum is divided by I_0. The normalized energy moments of the instrumental function and the moments of the inelastic spectrum together with the constant I_0 are saved in the file `dos.log`.

In order to subtract the elastic scattering, we consider the central part of the experimental spectrum between the first minimum points on the left and on the right. Let these points have energies $E_1 = -|E_1|$ and E_2 and intensities I_1 and I_2. The central part of the spectrum contains the elastic peak together with the inelastic contribution $I_{\rm in}(E)$. The latter must be approximated by a linear function at energy near $E = 0$. Therefore, at zero point $E = 0$ we may use a next approximation for $I_{\rm in}(0)$:

$$I_{\rm in}(0) = I_2 - \frac{I_2 - I_1}{E_2 - E_1}E_2. \tag{4.20}$$

After that the central elastic peak is subtracted according to

$$I(E) = I_t(E) - \alpha P(E), \tag{4.21}$$

where the constant α is determined by the condition $I(0) = I_{\rm in}(0)$,

$$\alpha = \frac{I_t(0) - I_{\rm in}(0)}{P(0)}. \tag{4.22}$$

Such a procedure allows one to subtract the elastic part and to maintain the contribution of inelastic scattering in the central part of the spectrum. However, this procedure often leads to significant fluctuations in the central part of the inelastic spectrum. In order to smooth the spectrum in the central part, an additional procedure may be performed. It replaces the central part by a polynominal of third degree that has the same values and the same first derivatives as the true spectrum at the points E_1 and E_2:

$$I(E) = I_1 + C_1(E - E_1) + C_2(E - E_1)^2 + C_3(E - E_1)^3, \quad E_1 < E < E_2, \tag{4.23}$$

where

$$C_1 = I_1', \quad C_2 = \frac{3F - GE_{21}}{E_{21}^2}, \quad C_3 = \frac{GE_{21} - 2F}{E_{21}^3}, \quad E_{21} = E_2 - E_1, \tag{4.24}$$

$$F = I_2 - I_1 - I_1'E_{21}, \quad G = I_2' - I_1', \quad I_1' = \left(\frac{{\rm d}I}{{\rm d}E}\right)_{E=E_1}, \quad I_2' = \left(\frac{{\rm d}I}{{\rm d}E}\right)_{E=E_2} \tag{4.25}$$

This procedure is performed if the parameter $K_{ey} = 1$. Note that such a procedure slightly changes the initial value of $I_{\rm in}(0)$, which leads to a new value of the Lamb–Mössbauer factor.

4.2.4. Lamb–Mössbauer factor

After subtraction of the elastic scattering contribution, the new normalization constant I_0 and the Lamb–Mössbauer factor $f_{\rm LM}$ are calculated using eqs. (4.8).

4.2.5. Practical implementation of deconvolution of the data and the instrumental function

In order to eliminate the multiple-phonon processes together with the instrumental function, Fourier images are calculated using FFT:

$$Q(\tau) = \int {\rm d}E \exp({\rm i}E\tau)P(E); \qquad J_0(\mathbf{k},\tau) = \int {\rm d}E \exp({\rm i}E\tau)I(E,\mathbf{k}). \tag{4.26}$$

Equation (4.10) cannot be used directly in a computer calculation, because the tails of the function $Q(\tau)$ have very small values (zero value at the points near the boundaries of the region). Therefore, the program uses the function $1/Q_0(\tau)$ instead of the function $1/Q(\tau)$, where

$$\frac{1}{Q_0(\tau)} = \frac{1+P_{\rm if}}{Q(\tau)+P_{\rm if}}. \tag{4.27}$$

Here the real value $P_{\rm if}$ is a parameter of the program. The function $Q(\tau)$ reaches a maximum at zero argument $Q(0) = 1$, because the instrumental function $P(E)$ is normalized to unity. One may see that if a user chooses $P_{\rm if} = 0.1$ the instrumental function will be almost completely deconvoluted by the program. On the other hand, if a user chooses $P_{\rm if} = 100$ the procedure will eliminate the multiple-phonon scattering but will not deconvolute the instrumental function because $Q_0(\tau) = 1$ with good accuracy. As a result, the function $J(\mathbf{k},\tau)$ is calculated as

$$J(\mathbf{k},\tau) = \frac{J_0(\mathbf{k},\tau)}{I_0 f_{\rm LM}(\mathbf{k})Q_0(\tau)}. \tag{4.28}$$

4.2.6. Intermediate arrays

To check the computing process, it is convenient to save the arrays used in the FFT procedures and to show them graphically. Since the total number of dots in the arrays is very large, the program stores only the central parts of the arrays and omits some intermediate dots. The results are written in the files `dos.h1`, `dos.h2`, `dos.h3`. The file `dos.h1` contains three functions: $I(E)$, $P(E)$ and $I_t(E)$. $P(E)$ and $I_t(E)$ are normalized to unity, while $I(E)$ is multiplied by the constant $C_{\rm s}$ (a parameter of the program) before storing so that the tails of the spectrum are clearly shown. The parameters $M_{\rm r}$ and $M_{\rm s}$ give half of the number (radius) of dots to be stored and the step between dots ($n = 1, 2$ or more, the number of intermediate dots to be omitted in the initial table is $n-1$). The file has four columns (the first one contains the number of dots in the initial table as an argument of the functions).

The file `dos.h2` has five columns: the first one is the same as in the preceding file, the second column contains (1/4) Re[$Q(\tau)$], the third column contains Im[$Q(\tau)$], the fourth column Re[$M(\tau)$] and the fifth column Im[$M(\tau)$]. These functions are results of the forward FFT projection. In order to distinguish them in the figure, we note that their imaginary parts are zero in the central point, and the instrumental function has a more smooth behaviour. The parameters K_r and K_s have the same meaning as the parameters M_r and M_s, but now for the file `dos.h2`.

The file `dos.h3` contains the results of the backward FFT projection. It has two columns: the first is the same as in `dos.h1`, the second contains the real function $D(E) = (E/E_\mathrm{R})(1 - \exp(-\beta E)) \int (\mathrm{d}\tau/2\pi) \exp(-\mathrm{i}E\tau) M(\tau)$ (see eq. (4.11)). It uses the same parameters as the file `dos.h1`.

4.2.7. Sum rules

The function PDOS is calculated from the table of the $D(E)$ function. The output table is written in the file `dos.dat`. It has two columns: the energy E in meV and the DOS $g(E)$ in $1/\mathrm{meV}$. The first value of E is always zero. The last (maximal) value of E is a parameter of the program named E_{gm}. The number of dots in the array N_g is also a parameter. The output values are obtained by linear interpolation of the $D(E)$ table. The output table is used for the calculation of the values of $G_n^{(d)}$ using eq. (4.12). On the other hand, the same values $G_n^{(m)}$ are calculated from the righthand sides of the formulas (4.13) and (4.14) taking into account eqs. (4.15), (4.16). The ratio $s_n = G_n^{(d)}/G_n^{(m)}$ is written in the file `dos.log` to check the mathematical accuracy of the procedure. Ideally, all values of s_n must be unity. However, since the instrumental function is not completely eliminated from the DOS, the values s_n are usually slightly different from unity. Finally, the mean kinetic energy (in meV) is calculated as $G_1^{(m)}/4$, and the mean force constant (in N/m) as $0.003833 M G_2^{(m)}$, where M is the mass of the nucleus (in atomic units). M and E_R are parameters of the program.

5. The structure of the computer program

The UNIX version of the program at the beamline ID-18 at the ESRF has been developed as a command batch-file `dos` which contains 5 lines (commands):

```
dtpad dos.par
dos.exe < dos.par
vkps
ghostview -a4 -magstep -1 dos.ps
dtpad dos.log
```

The first line runs the text editor `dtpad` for preparing the text file `dos.par` of the input data for the calculating part of the program `dos.exe`. Only the left-hand parts of the first five lines are essential. All other parts may be used for comments. The file may contain many different sets of input data. The program takes only the first set. Below the structure of the input data is described: The first line contains an arbitrary text in apostrophes. For example:

```
'Example 1: Fe polycrystalline sample'.
```

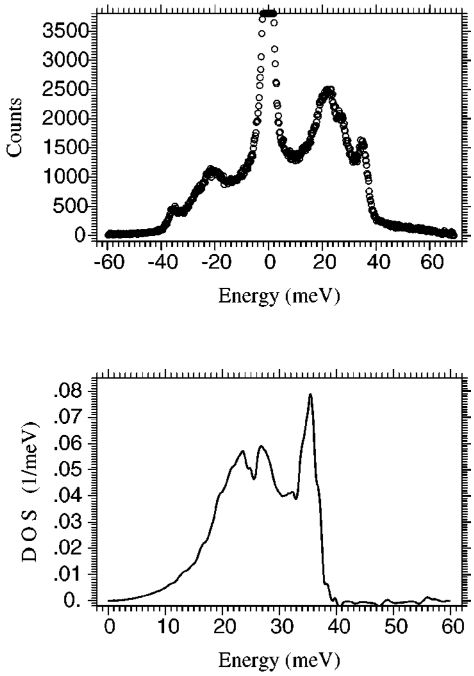

Figure 1. Example of a figure created by the program. Here the initial data (energy spectrum of inelastic nuclear absorption in iron, top), are shown together with calculated data (density of phonon states, bottom). The program also shows the following comment: Lamb–Mössbauer factor = 0.7777, mean kinetic energy = 15.762 meV; mean force constant = 146.37 n/m. Case 1: Fe polycristalline sample.

The text may contain up to 128 symbols. This text is a title of the examples, and it is shown at the bottom line of the output figure (see figure 1).

The second line contains the two names of the files with the data for the instrumental function and for the intensity of inelastic absorption. The names must be inputted with apostrophes. For example:

```
'mon17.dat' 'fer17.dat'
```

It is assumed that the files are located in the same directory.

The third line contains numerical values of two parameters in arbitrary format:

$$E_{gm} \text{ and } N_g$$

(see definitions above).

The fourth line contains

$$T \quad A_{\mathrm{p}} \quad P_{\mathrm{if}}.$$

Here T is the temperature (in K), while A_{p} and P_{if} are described above.

The fifth line contains the parameters

$$N_{\mathrm{si}} \quad P^{m}_{\mathrm{rms}} \quad P^{i}_{\mathrm{rms}} \quad N_b \quad N_m$$

as described above.

There is another file of input data, `dos.hc`, which contains the additional constants used permanently without changes. They may be changed separately by calling the editor `dtpad`. It contains three lines with the parameters

$$\begin{array}{llllll} E_{\mathrm{R}} & M_n & & & & \\ N & E_b & & & & \\ M_{\mathrm{r}} & M_{\mathrm{s}} & K_{\mathrm{r}} & K_{\mathrm{s}} & K_{ey} & C_{\mathrm{s}}. \end{array}$$

All parameters are described above.

After saving the data and closing the editor window, the second line of the command batch-file runs the program `dos.exe` which takes the data from the files `dos.hc` and `dos.par`. The program calculates the results and saves them in the files `dos.dat`, `dos.h1`, `dos.h2`, `dos.h3` and the text file `dos.log`. The program also writes the file `vkps.par` which is used by the program `vkps` for preparing the PostScript file of the figure showing the results in graphical form (figure 1). Also, the files `dos.dc1`, `dos.dc2` and `dos.vkp` are written in the current directory. These files may later be shown graphically with the command batch-file `dosh`. The command file `dos` does not show them.

The third command of the batch-file runs the program `vkps`. This program is a PostScript generator that makes PostScript files and allows one to create figures of different kinds using a set of simple instructions and data files of different kinds. The PostScript file has the name `dos.ps`. It may be used for printing figures as well as for looking for the results on the terminal's monitor using the program `ghostview.`

The fourth command of the batch file runs `ghostview` to see the output page on a screen.

The fifth command of the batch file runs `dtpad` with the file `dos.log` to see the validity of the sum rules and some additional information.

In order to control the procedure of data filtering for forward and backward Fourier transformation, one can consult the intermediate arrays, written in the files `dos.h1`, `dos.h2`, `dos.h3` (figure 2). The figure is not shown automatically. In order to see the figure one has to run the command batch-file `dosh`.

Appendix. An example of input and output data

Here we give an example to illustrate the performance of the program. The file `dos.par` has the following content:

```
‘Example 1:  Fe polycrystalline sample’.
‘mon17.dat’ ‘fer17.dat’
60. 501
295. 0. 0.1
7 100. 70. 100 8
```

The program `dos` creates and shows a PostScript file shown in figure 1. This output shows the experimental data and the calculated DOS, as well as some parameters

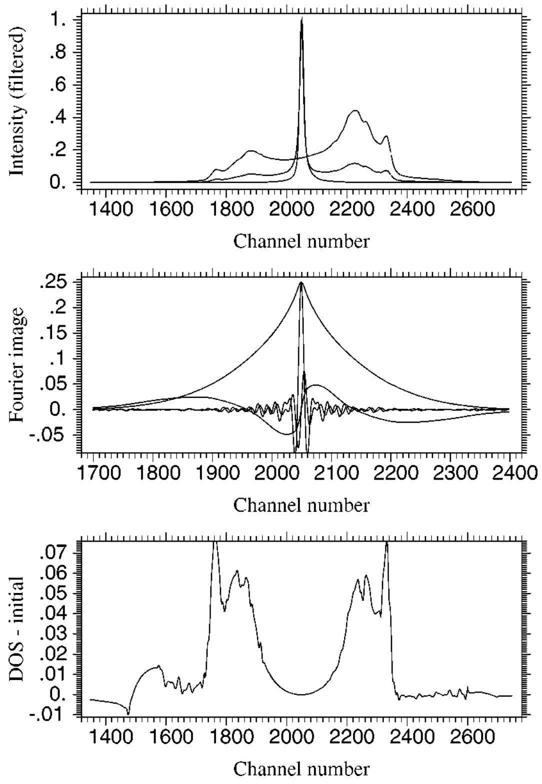

Figure 2. Intermediate arrays, which may be shown by the program `dosh`. The top, middle and bottom figures show the data of the files `dos.h1`, `dos.h2` and `dos.h3`, respectively (see text for the structure of these files).

derived from DOS. The intermediate arrays may be consulted using the program `dosh`. The resulting figure created by this program is shown in figure 2.

References

[1] E. Gerdau, R. Rüffer, H. Winkler, W. Tolksdorf, C.P. Klages and J.P. Hannon, Phys. Rev. Lett. 54 (1985) 835.

[2] T.S. Toellner, this issue, section VI-1.

[3] A.I. Chumakov and W. Sturhahn, this issue, section V-1.1.

[4] K.S. Singwi and A. Sjölander, Phys. Rev. 120 (1960) 1093.

[5] A.I. Chumakov, R. Rüffer, A.Q.R. Baron, H. Grünsteudel, H.F. Grünsteudel and V.G. Kohn, Phys. Rev. B 56 (1997) 10758.

[6] V.G. Kohn, A.I. Chumakov and R. Rüffer, Phys. Rev. B 58 (1998) 8437.

[7] W. Sturhahn and V.G. Kohn, this issue, section III-2.2.

[8] L. Van Hove, Phys. Rev. 95 (1954) 249.

[9] H.J. Lipkin, Ann. Physics (NY) 18 (1962) 182.